Adaptive quantile control for stochastic system

Citation for the original published paper (version of record):
Ma, X., Qian, F., Zhang, S. et al (2022). Adaptive quantile control for stochastic system. ISA Transactions, 123: 110-121. http://dx.doi.org/10.1016/j.isatra.2021.05.032

ISA Transactions xxx (xxxx) xxx

Contents lists available at ScienceDirect

ISA Transactions

journal homepage: www.elsevier.com/locate/isatrans

Research article

Adaptive quantile control for stochastic system

Xuehui Ma [a,1], Fucai Qian [a,2,*], Shiliang Zhang [b,3], Li Wu [a,4]

[a] School of Automation and Information Engineering, Xi'an University of Technology, China
[b] Department of Computer Science and Engineering, Chalmers University of Technology, Sweden

ARTICLE INFO

Article history:
Received 8 July 2020
Received in revised form 20 May 2021
Accepted 21 May 2021
Available online xxxx

Keywords:
Adaptive quantile control
Asymmetric Laplace Distribution
Bayesian quantile sum estimator
Certainty equivalence principle

ABSTRACT

Adaptive control has been successfully developed in deriving control law for stochastic systems with unknown parameters. The generation of reasonable control law depends on accurate parameter estimation. Recursive least square is widely used to estimate unknown parameters for stochastic systems; however, this approach only fits systems with Gaussian noises. In this paper, the adaptive quantile control is first proposed to cover the case where stochastic system noise follows sharp and thick tail distribution rather than Gaussian distribution. In the proposed approach, the system noise is modeled by the Asymmetric Laplace Distribution, and the unknown parameter is online estimated by our developed Bayesian quantile sum estimator, which combines recursive quantile estimations weighted by Bayesian posterior probabilities. With the real-time estimated parameter, the adaptive quantile control law is constructed based on the certainty equivalence principle. Our proposed estimator and controller are not computationally consuming and can be easily conducted in the Micro Controller Unit to fit practical applications. The comparison with some dominant controllers for the unknown stochastic system is conducted to verify the effectiveness of the adaptive quantile control.

1. Introduction

The random noises in some practical stochastic systems, e.g., economic system, social decision-making system, and biological ecosystem, usually have sharp, thick-tailed, and skewed characteristics, making them different from the commonly used white Gaussian noise [1,2]. This kind of noise will reduce the accuracy of the parameter estimation under Gaussian-assumed approaches, and consequently degrade the control performance for stochastic systems. This challenge impedes verities of control applications where, e.g., financial investors design a regulator to control financial risks better [3]; management of web or service industry makes more favorable decisions that satisfy most of the customers as possible rather than on average [4,5]; policymakers allocate resources according to wealth inequality between the urban and the rural [6], etc. The addressing of this challenge can promote the control of stochastic systems, e.g., economic or social decision-making systems, with a high capacity for handling uncertainties. In this paper, we consider the solution of adaptive control for stochastic systems with uncertainties, which includes unknown parameters and sharp, thick-tailed, skewed random noises.

Adaptive control is a potential way to tackle uncertainties in the control of stochastic systems. This method is concerned with designing a control law that provides desired system performance for the system under conditions of uncertainty, by the mean of tuning its parameters or structure to reduce the influence of uncertainty and improve the approximation of the desired system [7]. Generally, adaptive control approaches deal with uncertainties including unknown parameters and random noise [8,9]. For example, the model parameter self-tuning control with Recursive Least Square (RLS) or Kalman Filter (KF) as a recursive parameter estimator has been successfully applied in industrial control processes, where random noises are comparatively small, and model parameters are unknown [10–13]. Such a self-tuning approach consists of two components: (1) learning the unknown parameter of the stochastic system; (2) exerting the control signal on the stochastic system to guarantee that the output track a desirable trajectory [14,15]. Control strategies based on this approach are still widely applied for industrial control processes nowadays for its easy implementation on Micro Computer and

* Corresponding author.
E-mail addresses: maxuehuiyx@foxmail.com (X. Ma), qianfc@xaut.edu.cn (F. Qian), shiliang@chalmers.se (S. Zhang), wuliphd@stu.xaut.edu.cn (L. Wu).

1 Her research interest covers stochastic control, adaptive control, system identification, and flight control.

2 His research interest covers stochastic control, systems identification, nonlinear control, and large-scale systems.

3 His research interest covers privacy preservation, machine learning, modeling and data processing, and intelligent control.

4 His research interest covers type-2 fuzzy logic theory, artificial intelligence, intelligent control, and their applications in industry.

https://doi.org/10.1016/j.isatra.2021.05.032

Micro Controller Unit [16–19]. In recent years, model-free adaptive controllers are developed for unknown systems. For example, Kiumarsi et al. applied reinforcement learning algorithms for optimal tracking control of linear discrete-time systems with unknown dynamic matrices [20–22]. In Onder Tutsoy's work, an adaptive estimator was designed to learn the approximate Q-function and control policy for the unknown system with output error type random noise [23,24]. All of the above strategies assume that random noises in stochastic systems follow Gaussian distribution.

However, noises in some practical systems, e.g., social-economic system and biological ecosystem, might not follow Gaussian distribution. Instead, such systems suffer from sharp and thick-tailed noises [1,2], where the aforementioned control strategies with Gaussian-noise-assumption might no longer be efficient. Robust control serves as an alternative solution to tackle system uncertainties [25–27]. For example, Q-learning approximate dynamic programming, heuristic dynamic programming, and dual-heuristic dynamic programming were used to solve the zero-sum game related H-infinity optimal control problem for discrete-time linear systems with dynamic parameter matrices unknown [28–31]. Yi Jiang et al. designed an off-policy reinforcement learning approach to solve the output regulation problem for unknown linear discrete-time systems suffering disturbance [32]. This approach supposed that the disturbance is observable, which is difficult to satisfy in some practical system. Moreover, robust control methods consider the worst-case disturbance in systems, which induce quite conservative optimal control strategies.

Since the random noise with sharp and thick-tailed characteristics can be described by Asymmetric Laplace Distribution (ALD) [33–37], the single quantile regression is introduced to estimate model parameters for a system with ALD noise [38–40]. Nevertheless, it is difficult to choose the quantile in single quantile regression when the distribution of system noise is unknown. As an extension, researchers investigated approaches of composite quantile regression in model parameter estimation, which combines multiple quantile regressions. Zou et al. introduced an equally weighted composite quantile regression that combines multiple quantile regression models [41]. Zhao et al. calculated the different weights for different quantiles by minimizing the corresponding asymptotic variance [42]. Huang et al. proposed bayesian composite quantile regression, where the weight of each quantile is treated as an open parameter and estimated through Markov Chain Monte Carlo (MCMC) sampling procedure [43]. Most of the works on quantile regression are based on the MCMC method. However, the MCMC method is not suitable for parameter estimation in adaptive control, since it is conducted offline rather than updating model parameters in real-time.

In this paper, we aim to promote unknown stochastic system control with adaptive features, and more importantly, with the capacity to preserve control performance confronted with ALD noise in systems. To this end, an adaptive quantile control is presented for tracking control of linear discrete-time systems with unknown parameters and ALD noise. The proposed scheme contains two parts: (1) Bayesian quantile sum estimator (BQSE); (2) output tracking controller. The developed BQSE is a real-time recursive parameter estimator that estimates unknown parameters of the system suffered from ALD noise. Specifically, the BQSE combines multiple quantile estimators by summing each of the estimated parameters weighted by corresponding Bayesian posterior probabilities for different quantiles. The estimated parameters from BQSE are regarded as real parameters in the derivation of control law, which is based on the principle of certainty equivalence in stochastic systems. To verify our approach, we perform numerical experiments and the control

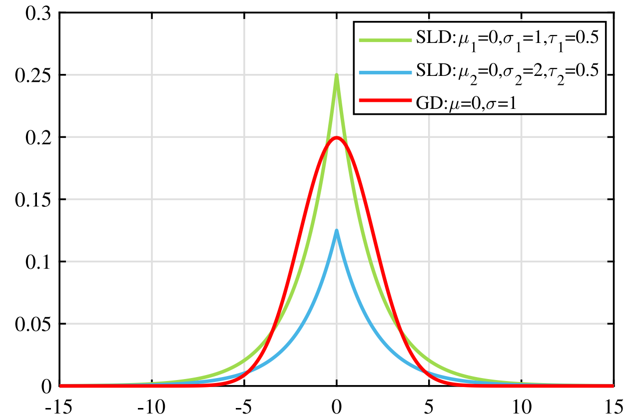

Fig. 1. The probability density function of Symmetric Laplace Distribution and Gaussian Distribution.

performance of the proposed method is compared with minimum variance control where the parameter is known, the traditional self-tuning control with RLS estimator [11], Q-leaning based output tracking control [20], reinforcement learning based control for output error system with an adaptive estimator [23,24], and adaptive dual model predicted control [19].

The rest of this paper is organized as follows. In Section 2, we present a stochastic system with ALD noise. The online BQSE and the adaptive quantile control law based on the certainty equivalence principle for ALD noise are described in Section 3. Section 4 provides numerical experiments to evaluate the performance of BQSE and the adaptive quantile controller. Conclusions are given in Section 5.

2. Problem statement

Consider a linear discrete-time, single-input and single-output, stochastic system [12]

$$\begin{aligned} A(z^{-1})y(k) &= B(z^{-1})u(k-d) + C(z^{-1})e(k) \\ k &= 0, 1, \ldots, N-1 \end{aligned} \tag{1}$$

where $y(k)$ is system output, $u(k)$ is control input. $A(z^{-1}) = 1 + \sum_{i=1}^{n} a_i z^{-i}$, $B(z^{-1}) = b_0 + \sum_{j=1}^{m} b_j z^{-i}, b_0 \neq 0$, $C(z^{-1}) = 1 + \sum_{i=1}^{n} c_i z^{-i}$. The parameters in $A(z^{-1}), B(z^{-1}), C(z^{-1})$ are unknown. The time delay d and the order n and m are assumed known. The random noise $e(k)$ follows ALD.

Firstly we show how Gaussian and Laplace noises differ from each other and the influence brought by this distinction. Suppose that the random variable x follows ALD and its probability density function is given by

$$f_{pdf}(x) = \frac{\tau(1-\tau)}{\sigma} \begin{cases} e^{-(1-\tau)\frac{|x-\mu|}{\sigma}}, x < \mu \\ e^{-\tau\frac{|x-\mu|}{\sigma}}, x \geq \mu \end{cases} \tag{2}$$

where $\tau \in (0, 1)$, $\mu \in (-\infty, \infty)$, and $\sigma > 0$ [44]. Fig. 1 shows the probability density function of Gaussian Distribution(GD, its mean is 0 and variance is σ) and Symmetric Laplace Distribution(SLD, its position parameter is $\mu = 0$, scale parameter is $\sigma_1 = 1, \sigma_2 = 2$, asymmetry parameter is $\tau = 0.5$). Compared with Gaussian Distribution, Laplace Distribution has the character of sharp peak and thick tail. Fig. 2 shows the probability density of ALD (its asymmetry parameter τ is not 0.5, $\tau_2 = 0.9, \tau_3 = 0.2, \tau_4 = 0.9$), where the curve of probability density function for ALD is asymmetric. An economic system or biological ecosystem generally follows the distribution with sharp-peak, thick-tailed and asymmetric features, like those in the ALD shown in Fig. 2.

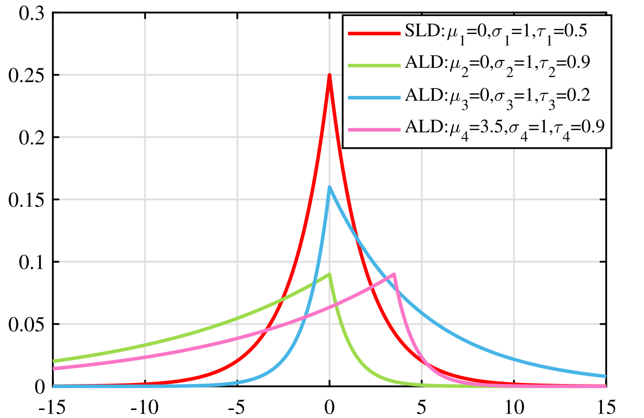

Fig. 2. The probability density function of Asymmetric Laplace Distribution ($\tau_2 = 0.9$, $\tau_3 = 0.2$, $\tau_4 = 0.9$).

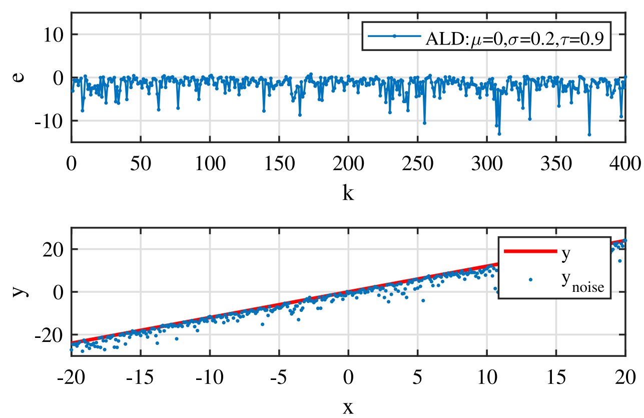

Fig. 3. Asymmetric Laplace Noise e with the asymmetry parameter $\tau = 0.9$ and the output of $y = 1.2x + e$.

The Cumulative Distribution Function of ALD is

$$F(x) = \int_{-\infty}^{x} f(t)dt = \begin{cases} \tau e^{\frac{(1-\tau)}{\sigma}(x-\mu)}, x < \mu \\ 1-(1-\tau)e^{-\frac{\tau}{\sigma}(x-\mu)}, x \geq \mu \end{cases} \tag{3}$$

The detailed derivation is shown in Appendix A.1.

The ALD noise is derived from the inverse function of ALD distribution function, and the inverse function is shown as

$$F^{-1}(x) = \begin{cases} \mu + \frac{\sigma}{1-\tau}\ln\frac{1}{\tau}x, 0 < x < \tau \\ \mu - \frac{\sigma}{\tau}\ln\frac{1}{1-\tau}(1-x), \tau \leq x < 1 \end{cases} \tag{4}$$

The detailed derivation is shown in Appendix A.2.

The upper part of Fig. 3 shows the ALD noise e with the asymmetry parameter τ is 0.9, the position parameter μ is 0, and the scale parameter σ is 0.2. It can be observed that most of the noise data locate under $x = 0$ while a few above it. y is the output of a simple linear model with ALD noise e added as $y = 1.2x + e$, as shown in the lower part of Fig. 3. Fig. 4 shows the ALD noise e with the asymmetry parameter is 0.15 and most of the noise data distribute above $x = 0$. Fig. 5 depicts the SLD noise e whose asymmetry parameter is 0.5. The noise data distribute symmetric around $x = 0$. Fig. 6 shows the White Gaussian Noise e with 0 mean, and variance σ is 0.2.

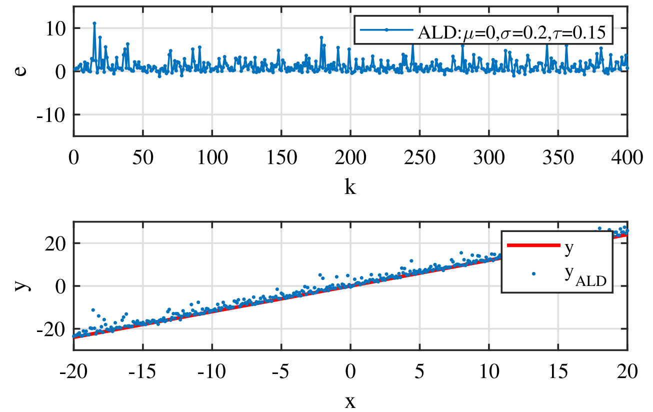

Fig. 4. Asymmetric Laplace Noise e with the asymmetry parameter $\tau = 0.15$ and the output of $y = 1.2x + e$.

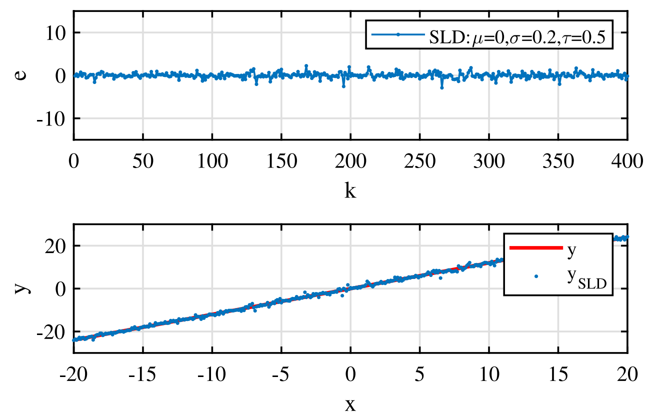

Fig. 5. Symmetric Laplace Noise e with the asymmetry parameter $\tau = 0.5$ and the output of $y = 1.2x + e$.

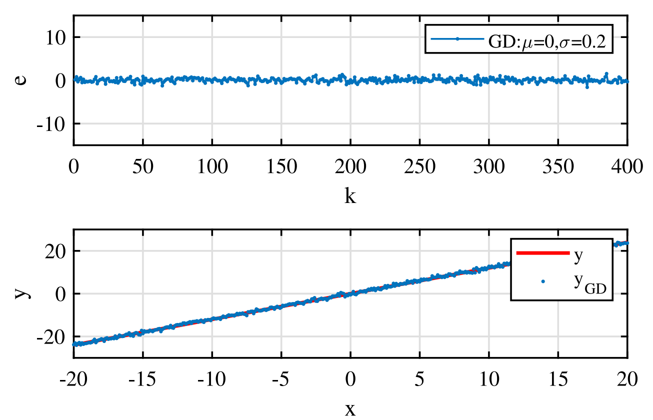

Fig. 6. White Gaussian Noise e and the output of $y = 1.2x + e$.

In the case of ALD, the expectation and variance are defined as μ_{Lap} and σ_{Lap}, respectively, and are calculated as:

$$\mu_{Lap} = \frac{\sigma(1-2\tau)}{\tau(1-\tau)} \qquad \sigma_{Lap} = \frac{\sigma^2(1-2\tau+2\tau^2)}{\tau^2(1-\tau)^2} \tag{5}$$

when the position parameter μ is set to 0. The detailed information on this calculation is shown in Appendix A.3.

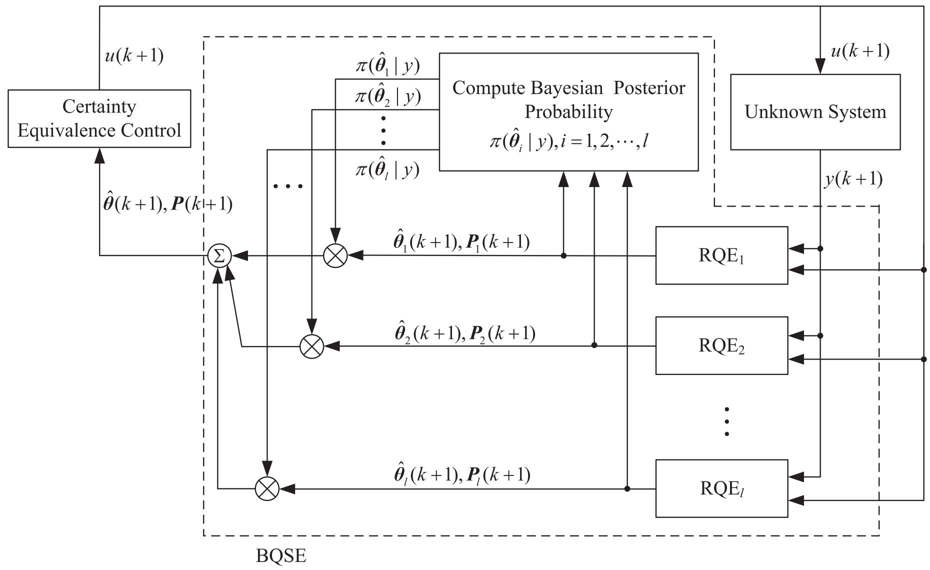

Fig. 7. Block diagram illustrating the adaptive quantile control with BQSE.

3. Controller design

This section details the controller design for adaptive quantile control with BQSE. The derivation and deformation of the model are shown in Section 3.1; the recursive quantile estimation (RQE) for single quantile estimation is described in Section 3.2; the Bayesian quantile sum estimation is explained in Section 3.3; the certainty equivalence control law is described in Section 3.4.

The block diagram of the proposed adaptive quantile control with BQSE is shown in Fig. 7. The unknown stochastic system in the figure can be described by the model with unknown parameters and ALD noises in Eq. (1). The estimator BQSE in the dashed line box provides real-time estimated parameters for the controller. The estimated parameters are regards as real parameters for the model to calculate the control law under the certainty-equivalence principle. In the BQSE, l single quantile estimators perform simultaneously, and each of them generates an estimated parameter $\hat{\boldsymbol{\theta}}_i$. The desired estimated parameters $\hat{\boldsymbol{\theta}}$ are the sum of all the $\hat{\boldsymbol{\theta}}_i$ weighted by Bayesian posterior probability.

3.1. Derivation and deformation of the model

The adaptive quantile controller is based on the classical self-tuning control proposed by Clarke and Gawthrop [11]. This control strategy can be applied to minimum phase and non-minimum phase systems by selecting appropriate parameters in the auxiliary system. Assume that the auxiliary output of the system in Eq. (1) is

$$y_a(k) = P(z^{-1})y(k) + Q(z^{-1})u(k-d) - R(z^{-1})y_r(k) \tag{6}$$

where $y_r(k)$ is reference signal, $P(z^{-1}) = p_0 + \sum_{i=1}^{n_p} p_i z^{-i}$, $Q(z^{-1}) = 1 + \sum_{i=1}^{n_q} q_i z^{-i}$, $R(z^{-1}) = 1 + \sum_{i=1}^{n_r} r_i z^{-i}$. Introducing equation $P(z^{-1})C(z^{-1}) = A(z^{-1})L(z^{-1}) + z^{-d}G(z^{-1})$ and combining equations (1) and (6) results in

$$\begin{aligned} C(z^{-1})y_a(k+d) = F(z^{-1})u(k) + G(z^{-1})y(k) + H(z^{-1})y_r(k+d) \\ + C(z^{-1})\bar{e}(k+d) \end{aligned} \tag{7}$$

where $F(z^{-1}) = Q(z^{-1})C(z^{-1}) + B(z^{-1})L(z^{-1})$, $H(z^{-1}) = -C(z^{-1})R(z^{-1})$, $\bar{e}(k) = L(z^{-1})e(k)$. The detailed derivation of Eq. (7) is shown in Appendix A.4. The roots of characteristic polynomial $D(z^{-1}) = P(z^{-1})B(z^{-1}) + Q(z^{-1})A(z^{-1})$ should be located inside unit circle on z-plane for the stability of system, which can be provided by selecting the appropriate $P(z^{-1})$ and $Q(z^{-1})$. Let $\boldsymbol{\theta}^T = [f_0, f_1, \ldots, f_{n_f}, g_0, g_1, \ldots, g_{n_g}, h_0, h_1, \ldots, h_{n_h}]$ be the vector of unknown parameters, and the system in Eq. (7) can be rewritten as

$$y_a(k+1) = \boldsymbol{\Phi}^T(k)\boldsymbol{\theta}(k) - y_r(k+1) + \bar{e}(k+1) \tag{8}$$

where $\boldsymbol{\Phi}^T(k) = [u(k), \ldots, u(k-n_f), y(k), \ldots, y(k-n_g), y_r(k); \ldots; y_r(k-n_h)]$, $\bar{e}(k)$ is ALD noise with asymmetry parameter $\bar{\tau}$. For ease of exposition in the following content, time delay d is set to 1 and $C(z^{-1}) = 1$.

3.2. Recursive quantile estimation

The RLS estimator is an unbiased estimator with minimum variance and is applicable for the system with white Gaussian noise; however, its performance is poor in non-Gaussian, especially in sharp or thick-tail noise scenarios [37]. Extensive literature indicated that noise distributions with sharp and thick tail are more common than Gaussian distributions in practice. Roger Koenker proposed Quantile Regression, which has been widely leveraged in non-Gaussian noise distribution cases [45]. However, this method is based on MCMC sampling approaches, e.g., Metropolis–Hastings and Gibbs samplings, which are not suitable for real-time control processes. Extension on quantile regression is necessary to gain the adaptive feature that is capable of estimating model parameters in real-time. To this end, a recursive quantile estimator, which is the basic component for the construction of the BQSE, is introduced in this section.

Given random variable Φ, the conditional cumulative distribution function of Y is $F_{Y|\Phi}(y)$, and the τth $(0 < \tau < 1)$ conditional quantile of Y is defined as

$$Q_\tau(y|\Phi) = \inf_y \{y : F_{Y|\Phi}(y) \geqslant \tau\} \tag{9}$$

where $\inf(\cdot)$ is infimum function. Consider the linear model in Eq. (8) with n samples

$$y(k+1) = \boldsymbol{\Phi}^T(k)\boldsymbol{\theta}(k) + e(k+1), k = 1, 2, \ldots, n \tag{10}$$

where $(\boldsymbol{\Phi}(k), y(k+1))$ is an observation sample, $e(k+1)$ is the noise whose τth quantile is supposed to be zero. The τth conditional quantile of $y(k+1)$ can be specified as $Q_\tau\{y(k+$

$1)|\Phi(k)\} = \Phi^T(k)\theta_\tau(k)$. The τth quantile estimation of θ is resolved by minimizing the loss function

$$\sum_{k=1}^{n} \rho_\tau\{y(k+1) - \Phi^T(k)\theta_\tau(k)\} \tag{11}$$

where

$$\rho_\tau(u) = \begin{cases} \tau u^2, & u \geqslant 0 \\ (\tau-1)u^2, & u < 0 \end{cases} \tag{12}$$

The minimization of Eq. (11) can be rewritten as

$$\begin{aligned} \theta_\tau = \arg\min \sum_{k=1}^{n} \Bigg[&(1-\tau) \sum_{y(k+1)<\Phi^T(k)\theta(k)} (y(k+1) \\ &- \Phi^T(k)\theta(k))^2 + \tau \sum_{y(k+1)\geq\Phi^T(k)\theta(k)} (y(k+1) \\ &- \Phi^T(k)\theta(k))^2 \Bigg] \end{aligned} \tag{13}$$

Eq. (13) is a piecewise quadratic function, and the solution of Eq. (13) yields the proposed RQE, which can be calculated iteratively as:

$$\begin{aligned} \mathbf{K}(k+1) &= \mathbf{P}(k)\Phi(k)[\lambda(k) + \Phi^T(k)\mathbf{P}(k)\Phi(k)]^{-1} \\ \hat{\theta}(k+1) &= \hat{\theta}(k) + \mathbf{K}(k+1)[y(k+1) - \hat{\theta}^T(k)\Phi(k)] \\ \mathbf{P}(k+1) &= [I - \mathbf{K}(k+1)\Phi^T(k)]\mathbf{P}(k) \end{aligned} \tag{14}$$

where

$$\lambda(k) = \begin{cases} 1/(1-\tau), y(k+1) < \hat{\theta}^T(k)\Phi(k) \\ 1/\tau, y(k+1) \geq \hat{\theta}^T(k)\Phi(k) \end{cases} \tag{15}$$

The detailed derivation of Eqs. (14) and (15) is shown in Appendix A.5.

3.3. Bayesian quantile sum estimation

According to Section 3.2, we will get different estimated parameters by setting the asymmetry parameter τ. Nevertheless, it is difficult to find an optimal τ since the distribution of noise is unknown. In this subsection, we proposed the BQSE that combines information of multiple recursive quantile estimators into one robust parameter estimator. In the BQSE, each individual recursive quantile estimator is assigned with a weight calculated by Bayesian posterior probability before being integrated to generate the final estimator.

The BQSE estimates $\hat{\theta}$ by solving the loss function

$$\begin{aligned} \hat{\theta} = \arg\min \sum_{i=1}^{m}\sum_{k=1}^{n} \Bigg[&(1-\tau_i) \sum_{y(k+1)<\Phi^T(k)\theta(k)} (y(k+1) \\ &- \Phi^T(k)\theta(k))^2 + \tau_i \sum_{y(k+1)\geq\Phi^T(k)\theta(k)} (y(k+1) \\ &- \Phi^T(k)\theta(k))^2 \Bigg] \end{aligned} \tag{16}$$

where $0 < \tau_1 < \tau_2 < \cdots < \tau_i < \cdots < \tau_m < 1$. It is difficult to solve the minimum of function (16) directly. According to Eq. (14), we can firstly get the estimated parameter $\hat{\theta}_i$ for each τ_i, and then obtain the integrated estimation of parameter $\hat{\theta}$ as the sum of every quantile estimated parameter $\hat{\theta}_i$ with conditional posterior probabilities as their weights.

The conditional posterior probability is based on the principle of Bayesian posterior probability. Given observations $\mathbf{y} = \{y_1, y_2, \ldots, y_n\}$, the conditional probability of θ for $\mathbf{y}$ is defined as $\pi(\theta|\mathbf{y})$. According to bayesian posterior probability, $\pi(\theta|\mathbf{y})$ can be written as

$$\pi(\theta|\mathbf{y}) = \frac{f_{pdf}(\mathbf{y}|\theta)\pi(\theta)}{\int_\Theta f_{pdf}(\mathbf{y}|\theta)\pi(\theta)d\theta} \tag{17}$$

where Θ is parameter space, $\pi(\theta)$ is the prior distribution of θ, $f_{pdf}(\mathbf{y}|\theta)$ is the probability density function of the model.

The discrete posterior distribution can be defined as

$$\pi(\theta_i|\mathbf{y}) = \frac{f_{pdf}(\mathbf{y}|\theta_i)\pi(\theta_i)}{\sum_i f_{pdf}(\mathbf{y}|\theta_i)\pi(\theta_i)} \tag{18}$$

where $\pi(\theta_i), i = 1, 2, \ldots, m$ is prior distribution sequence, $f_{pdf}(\mathbf{y}|\theta_i)$ has the form

$$\begin{aligned} &f_{pdf}(\mathbf{y}|\theta_i) \\ &= \tau_i(1-\tau_i) \begin{cases} e^{-(1-\tau_i)\|\mathbf{y}-\Phi^T\theta_i\|}, (\mathbf{y} - \Phi^T\theta_i) < 0 \\ e^{-\tau_i\|\mathbf{y}-\Phi^T\theta_i\|}, (\mathbf{y} - \Phi^T\theta_i) \geq 0 \end{cases} \end{aligned} \tag{19}$$

According to Eqs. (14) and (16), the iterative process for estimation of parameter θ_i under the asymmetry parameter τ_i is

$$\begin{aligned} \mathbf{K}_i(k+1) &= \mathbf{P}_i(k|k)\Phi(k)[\lambda_i(k) + \Phi^T(k)\mathbf{P}_i(k)\Phi(k)]^{-1} \\ \hat{\theta}_i(k+1) &= \hat{\theta}_i(k) + \mathbf{K}_i(k+1)[y(k+1) - \hat{\theta}_i^T(k)\Phi(k)] \\ \mathbf{P}_i(k+1) &= [I - \mathbf{K}_i(k+1)\Phi^T(k)]\mathbf{P}_i(k) \end{aligned} \tag{20}$$

where

$$\lambda_i(k) = \begin{cases} 1/(1-\tau_i), y(k+1) < \hat{\theta}_i^T(k)\Phi(k) \\ 1/\tau_i, y(k+1) \geq \hat{\theta}_i^T(k)\Phi(k) \end{cases} \tag{21}$$

The BQSE for θ is

$$\hat{\theta}(k) = \sum_{i=1}^{m} \pi(\hat{\theta}_i|\mathbf{y})\hat{\theta}_i(k) \tag{22}$$

the covariance matrix $\mathbf{P}(k+1)$ is

$$\mathbf{P}(k+1) = \sum_{i=1}^{m} \pi(\hat{\theta}_i|\mathbf{y})\mathbf{P}_i(k) \tag{23}$$

The structure of BQSE is shown in the dashed lines of Fig. 7.

3.4. Certainty equivalence control

The Certainty Equivalence (CE) control is based on the analysis of stochastic systems [46–48]. In CE control, the estimated parameters in Section 3.3 are regarded as real model parameters when calculating the control law. This method's advantage is that it can estimate the model parameters and calculate the control law simultaneously for the stochastic system.

The control law u^* at the kth time instant relies on the minimization of the output variance

$$u^*(k) = \arg\min_{u(k)} E\left\{[y_a(k+1)]^2|\theta_k, \Im_k, u(k)\right\} \tag{24}$$

where $y_a(k+1)$ is the auxiliary output signal at the $(k+1)$th instant, θ_k is system parameter, $\Im_k$ is historical information which is known and measurable

$$\Im_k = \{u(1), \ldots, u(k-1), y(1), \ldots, y(k)\}, \tag{25}$$

The system in Eq. (8) at the $(k+1)$th instant is rewritten as

$$y_a(k+1) = f_0(k)u(k) + \alpha^T(k)\varphi(k) + \bar{e}(k+1) \tag{26}$$

where parameter vector $\boldsymbol{\theta}(k)$ and observation vector $\boldsymbol{\Phi}(k)$ are partitioned as

$$\boldsymbol{\theta}^T(k) = \left[f_0(k) \;\vdots\; \boldsymbol{\alpha}^T(k) \right] \tag{27}$$

$$\boldsymbol{\Phi}^T(k) = \left[u(k) \;\vdots\; \boldsymbol{\varphi}^T(k) \right] \tag{28}$$

Combine the cost function (24) and the system in Eq. (26)

$$\begin{aligned} J(k) =& E\left\{[y_a(k+1)]^2 | \boldsymbol{\theta}_k, \Im_k, u(k)\right\} \\ =& E\left\{[f_0(k)u(k) + \boldsymbol{\alpha}^T(k)\boldsymbol{\varphi}(k) - y_r(k+1) \right. \\ & \left. + \bar{e}(k+1)]^2 | \boldsymbol{\theta}_k, \Im_k, u(k)\right\} \end{aligned} \tag{29}$$

In CE control principle, the estimated parameters $\hat{f}_0(k)$ and $\hat{\boldsymbol{\alpha}}^T(k)$ are equal to the real parameters. As a result, the real parameter in cost function is replaced by estimations and shown as

$$\begin{aligned} J(k) =& E\left\{[\hat{f}_0(k)u(k) + \hat{\boldsymbol{\alpha}}^T(k)\boldsymbol{\varphi}(k) - y_r(k+1) \right. \\ & \left. + \bar{e}(k+1)]^2 | \Im_k, u(k)\right\} \end{aligned} \tag{30}$$

Calculate the expectation in Eq. (30)

$$\begin{aligned} J(k) =& E\left\{[\hat{f}_0(k)u(k) + \hat{\boldsymbol{\alpha}}^T(k)\boldsymbol{\varphi}(k) - y_r(k+1)]^2\right\} \\ &+ E\left\{2[\hat{f}_0(k)u(k) + \hat{\boldsymbol{\alpha}}^T(k)\boldsymbol{\varphi}(k) - y_r(k+1)]\bar{e}(k+1)\right\} \\ &+ E\left\{\bar{e}^2(k+1)\right\} \\ =& [\hat{f}_0(k)u(k) + \hat{\boldsymbol{\alpha}}^T(k)\boldsymbol{\varphi}(k) - y_r(k+1)]^2 \\ &+ 2[\hat{f}_0(k)u(k) + \hat{\boldsymbol{\alpha}}^T(k)\boldsymbol{\varphi}(k) - y_r(k+1)]\mu_{Lap} \\ &+ \sigma_{Lap} \end{aligned} \tag{31}$$

where μ_{Lap} is the mean of $\bar{e}(k+1)$ and σ_{Lap} is its variance.

The control law can be obtained from the differential of $J(k)$ in Eq. (31)

$$\begin{aligned} \frac{\partial J(k)}{\partial u(k)} =& 2\hat{f}_0(k)[\hat{f}_0(k)u(k) + \hat{\boldsymbol{\alpha}}^T(k)\boldsymbol{\varphi}(k) - y_r(k+1)] \\ &+ 2\hat{f}_0(k)\mu_{Lap} = 0 \end{aligned} \tag{32}$$

and then we obtain the CE control law $u^*(k)$ as

$$u^*(k) = \frac{y_r(k+1) - \hat{\boldsymbol{\alpha}}^T(k)\boldsymbol{\varphi}(k) - \mu_{Lap}}{\hat{f}_0(k)} \tag{33}$$

where $\mu_{Lap} = \{\sigma(1-2\tau)\}/\{\tau(1-\tau)\}$, $\tau = \sum_{i=1}^{m} \pi(\hat{\boldsymbol{\theta}}_i|\boldsymbol{y})\hat{\tau}_i$.

4. Experiment implementation

In this section, the proposed adaptive quantile control is implemented and verified in comparison with five stochastic system controllers. Detailedly, the parameter estimation performance of BQSE is tested in Section 4.1; the performance of the adaptive quantile controller for minimum-phase and nonminimum-phase systems is tested in Sections 4.2 and 4.3, respectively. The comparisons of different control strategies are shown in Section 4.4.

Table 1 summarizes the implementation procedures of the proposed approach for clarity, and detailed settings of those procedures are shown in the following contents.

Table 1
The procedure of adaptive quantile control with BQSE.

Initialization: Initialize the parameter vector $\boldsymbol{\theta}_i(1)$, history information $\Im_1$, covariance $P_i(1)$, Bayesian posterior probability $\pi_i(1)$, and asymmetry parameter τ_i $*^1$.
Computation: (1) Estimate $\hat{\boldsymbol{\theta}}_i(k+1)$ based on Eq. (15) at iteration $k+1$ for every asymmetry parameter τ_i; (2) Calculate Bayesian posterior probability $\pi(\boldsymbol{\theta}_i|\boldsymbol{y})$ based on Eq. (13) at iteration $k+1$; (3) Calculate $\hat{\boldsymbol{\theta}}(k+1)$ and $\boldsymbol{P}(k+1)$ at iteration $k+1$ using Eqs. (17) and (18); (4) Calculate the control law $u^*(k+1)$ in Eq. (28) $*^2$; (5) $*^3$.
Notice: $*^1$: The initial value of Bayesian posterior probabilities should be summed up to 1. The value of asymmetry parameter is best to distribute in interval (0, 1) uniformly. $*^2$: The expectation of asymmetric laplace noise in Eq. (18) is updated in every iteration. The asymmetry parameter τ in μ_{Lap} is updated by $\sum_{i=1}^{m} \pi(\hat{\boldsymbol{\theta}}_i|\boldsymbol{y})\hat{\tau}_i$. $*^3$: Apply $u^*(k+1)$ for the control process and repeat step (1) to step (4) in every iteration.

4.1. BayesIan quantile sum estimator

In this subsection, simulations are conducted to compare the model parameter estimation performance of BQSE (with τ unknown) with RLS and RQE (with τ known). The tested samples are generated by exerting control signal sequence into a system described in Eq. (1) with parameters

$$\begin{aligned} & a_1 = -1.41, \quad a_2 = 0.9, \quad n = 2, \\ & b_0 = 0.5, \quad m = 0, \quad d = 1, \\ & \sigma = 0.02, \quad \tau = 0.9, \quad \mu = 0. \end{aligned} \tag{34}$$

The exerted control signal is set by $u(k) = [y_r(k+1) - a_1 y(k) - a_2 y(k-1)]/b_0$, where y_r is a 0.1 Hz square wave filtered by transfer function $1/(s+1)$. The ALD noise $e(k)$ added into this system is set as

$$e(k) = \begin{cases} \mu + \frac{\sigma}{1-\tau} \ln \frac{1}{\tau} x(k), 0 < x(k) < \tau \\ \mu - \frac{\sigma}{\tau} \ln \frac{1}{1-\tau}(1 - x(k)), \tau \le x(k) < 1 \end{cases} \tag{35}$$

where $x(k)$ is uniform distribution. We collected 100 samples of $\{u(k), y(k)\}$ for the parameter estimation simulation.

The initial parameter is set as $\boldsymbol{\theta}_i^T(1) = [0.1, 0.1, 0.1]$, and the initial $\boldsymbol{P}_i$ is $\boldsymbol{P}_i(1) = 100\boldsymbol{I}$. The initial Bayesian posterior probabilities for different asymmetry parameters τ_i are set as $\{\tau_1 = 0.9, \pi_1(1) = 1/9\}$, $\{\tau_2 = 0.8, \pi_2(1) = 1/9\}$, $\{\tau_3 = 0.7, \pi_3(1) = 1/9\}$, $\{\tau_4 = 0.6, \pi_4(1) = 1/9\}$, $\{\tau_5 = 0.5, \pi_5(1) = 1/9\}$, $\{\tau_6 = 0.4, \pi_6(1) = 1/9\}$, $\{\tau_7 = 0.3, \pi_7(1) = 1/9\}$, $\{\tau_8 = 0.2, \pi_8(1) = 1/9\}$, $\{\tau_9 = 0.1, \pi_9(1) = 1/9\}$, where Bayesian posterior probabilities are summed up to 1.

Fig. 8 shows the estimation of system output with different parameter estimation methods. The system output $y(k)$ is predicted based on real-time estimated parameters $\boldsymbol{\theta}$ at the kth iteration. In the legend of Fig. 8, 'Samples' denotes the generated sample, 'real' represents the samples from the real model without noises, 'RLS' means Recursive Least Squares, 'RQE' denotes Recursive Quantile Estimation with $\tau = 0.9$, and 'BQSE' is the proposed Bayesian Quantile Sum Estimator with τ unknown. Since the RQE is configured with exactly real asymmetry parameter, RQE is regarded as the ideal and benchmark estimator in this simulation. The estimated outputs from RQE and BQSE are closer to real ones than those from RLS. The curve of BQSE coincides with that of RQE about 15 iterations after the beginning of the iteration, which indicates the Bayesian posterior probability of BQSE converged at the 15th iterations. Fig. 9 shows the convergence of Bayesian posterior probability for different asymmetry parameters in BQSE. The posterior probability π_1 with $\tau = 0.9$ converged to 1 after 15 iterations, and the other posterior probabilities converged to 0.

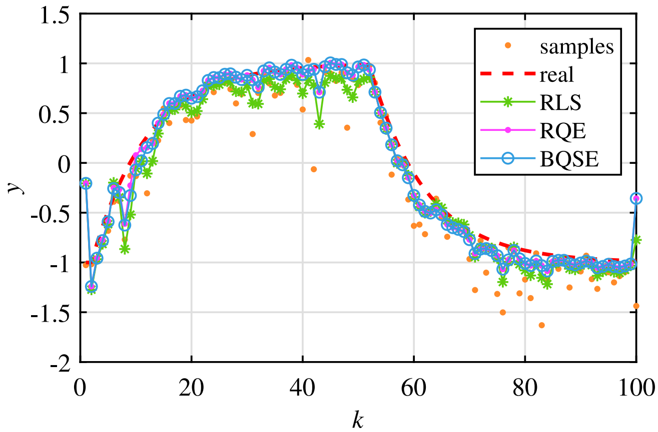

Fig. 8. The estimation of system output for RLS, RQE and BQSE.

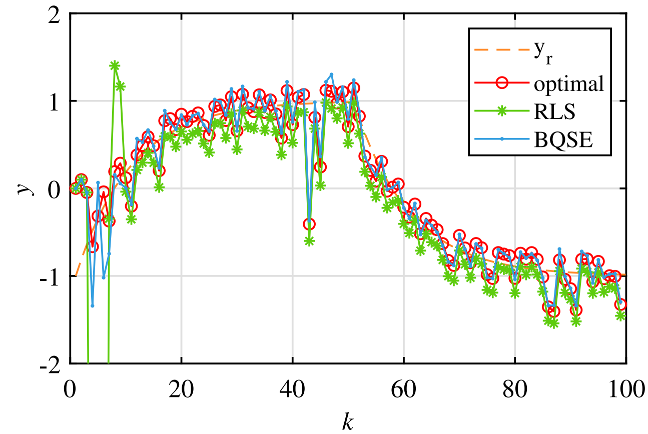

Fig. 10. The system output for optimal control, RLS and BQSE.

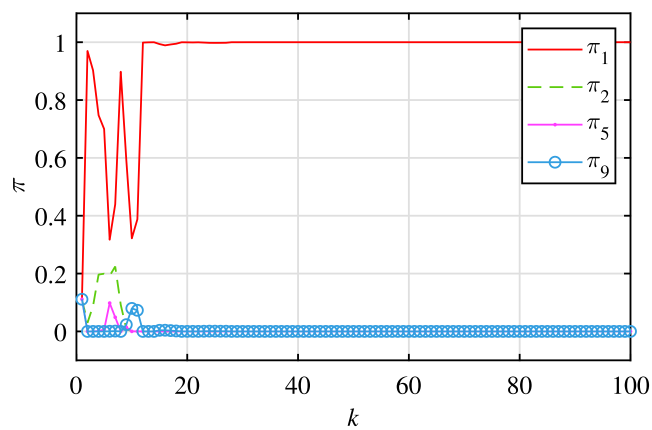

Fig. 9. The Bayesian posterior probability for different τ.

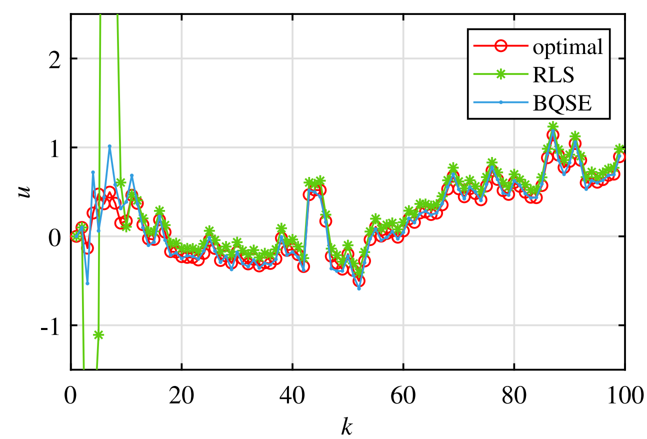

Fig. 11. The control signal of optimal control, RLS and BQSE.

Table 2
Comparison of three estimation methods.

Estimation method	Average performance
RLS	0.0620
RQE	0.0242
BQSE	0.0380

Table 2 shows the average of 1000 Monte Carlo simulation results for estimation performance. The performance for estimation in one single simulation is evaluated as accumulated error

$$V = \frac{1}{N}\sum_{k=1}^{N}[y_{est}(k) - y_{real}(k)]^2, \tag{36}$$

where y_{est} is the estimated output for different methods, N is the simulation length. The accumulated error V for ith Monte Carlo simulation is denoted as $V(i)$. The average accumulated error of M Monte Carlo simulation is computed as

$$\overline{V} = \frac{1}{M}\sum_{i=1}^{M} V(i). \tag{37}$$

The results shown in Table 2 show that the average accumulated error of BQSE is lower than RLS and is closer to RQE, which means BQSE converges to the real asymmetry parameter.

4.2. Adaptive quantile control for minimum-phase system

The following simulation is carried out for a minimum-phase system. This simulation illustrates how the considered adaptive quantile controllers perform. We compare the control performance of BQSE based adaptive quantile control with RLS based self-tuning control and optimal control. Since the optimal control is configured with exactly real model parameters, it is treated as the ideal and benchmark controller in this simulation. Consider a minimum-phase system described in Eq. (1) with parameters as:

$$\begin{aligned} &a_1 = -1.7, \quad a_2 = 0.7, \quad n = 2, \\ &b_0 = 1, \quad b_1 = 0.5, \quad m = 1, \quad d = 1, \\ &\sigma = 0.01, \quad \tau = 0.95, \quad \mu = 0. \end{aligned} \tag{38}$$

The reference signal y_r is a 0.1 Hz square wave filtered by transfer function $1/(s+1)$. The initial parameter is set as $\boldsymbol{\theta}_i^T(1) = [1, 1, 1, 1]$, and the initial $\boldsymbol{P}$ is $\boldsymbol{P}(1) = 100\boldsymbol{I}$. The initial control signal is set to $u(1) = 0.1$. The initial Bayesian posterior probability is set as $\{\tau_1 = 0.95, \pi_1(1) = 0.1\}$, $\{\tau_2 = 0.85, \pi_2(1) = 0.1\}$, $\{\tau_3 = 0.75, \pi_3(1) = 0.1\}$, $\{\tau_4 = 0.65, \pi_4(1) = 0.1\}$, $\{\tau_5 = 0.55, \pi_5(1) = 0.1\}$, $\{\tau_6 = 0.45, \pi_6(1) = 0.1\}$, $\{\tau_7 = 0.35, \pi_7(1) = 0.1\}$, $\{\tau_8 = 0.25, \pi_8(1) = 0.1\}$, $\{\tau_9 = 0.15, \pi_9(1) = 0.1\}$, $\{\tau_{10} = 0.05, \pi_{10}(1) = 0.1\}$.

Fig. 10 shows the system output y for optimal control, RLS, and BQSE, respectively. The system output for BQSE well tracked the reference signal y_r and converged to the output of optimal control within 20 iterations. Fig. 11 shows the control signal from the different control approaches, where the control signal of BQSE is closer to optimal control than that of RLS. Fig. 12 shows the convergence of Bayesian posterior probability π for BQSE. The

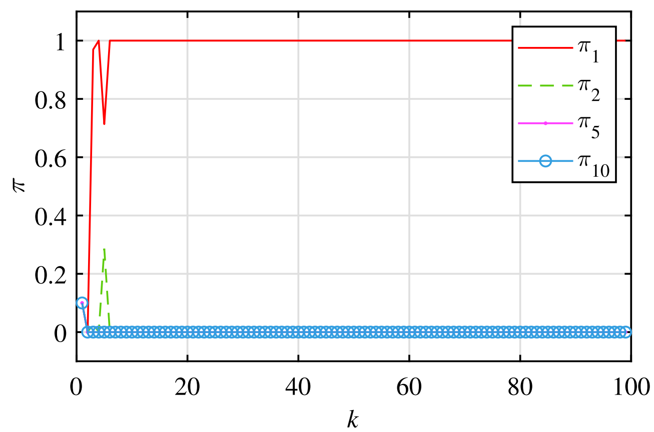

Fig. 12. The Bayesian posterior probability.

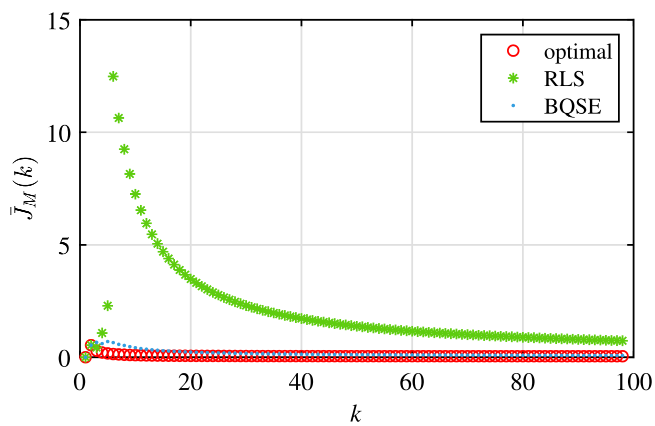

Fig. 13. The average control tracking performance index of 100 Monte Carlo simulations.

posterior probability $\pi_1$with parameter $\tau_1 = 0.95$ converged to 1, and other posterior probabilities converged to 0 soon after the control iterations begin.

To quantitatively investigate control tracking performance, we define the performance index as following

$$J = \frac{1}{N}\sum_{k=1}^{N}[y(k) - y_r(k)]^2. \tag{39}$$

where $y(k)$ and $y_r(k)$ are system output and reference signal at the kth iteration respectively, and N is the simulation length. The performance index J for ith Monte Carlo simulation is denoted as $J(i)$. With M Monte Carlo running, the average performance index is set as

$$\bar{J} = \frac{1}{M}\sum_{i=1}^{M} J(i). \tag{40}$$

where $\bar{J}(k)$ is the average performance index at the kth iteration.

Fig. 13 shows the average of 100 Monte Carlo simulation results for BQSE, RLS, and optimal control in every control iteration. The average control cost for BQSE is closer to optimal control than that of RLS. Table 3 shows the average tracking performance index at the 100th iteration. The performance index of adaptive quantile control with BQSE is closer to optimal control than RLS.

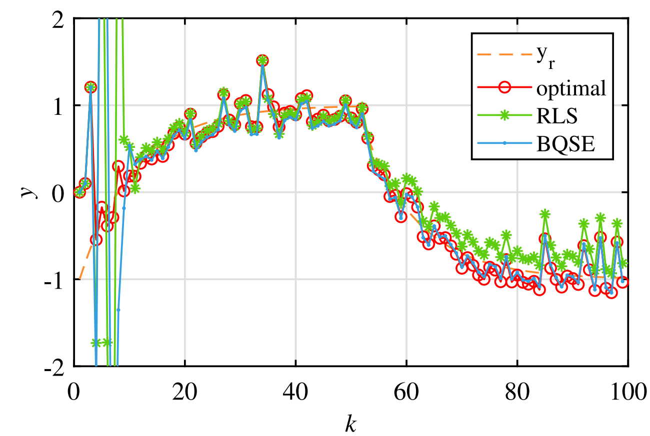

Fig. 14. The output of optimal control, RLS and BQSE.

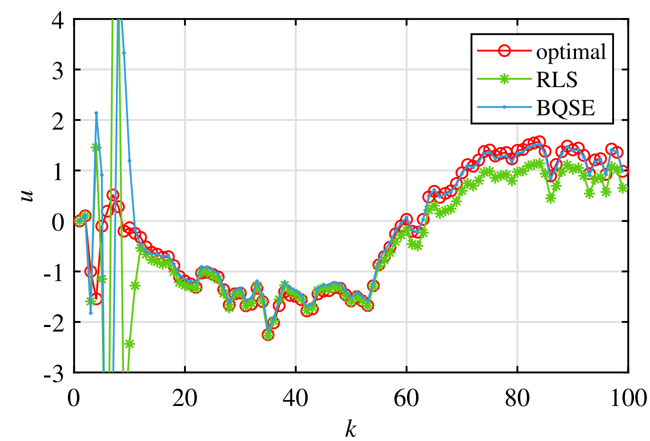

Fig. 15. The control signal of optimal control, RLS and BQSE.

Table 3
Comparison of three controller.

Estimation method	Average performance index
Optimal	0.0460
RLS	0.9703
BQSE	0.3546

4.3. Adaptive quantile control for nonminimum-phase system

Consider the nonminimum-phase system described in Eq. (1) with parameters as:

$$\begin{aligned} &a_1 = -2, \quad a_2 = 0.7, \quad n = 2, \\ &b_0 = 1, \quad b_1 = 2, \quad m = 1, \quad d = 1, \\ &\sigma = 0.02, \quad \tau = 0.2, \quad \mu = 0. \end{aligned} \tag{41}$$

The initial value of different quantile and the corresponding initial Bayesian posterior probability is set as $\{\tau_1 = 0.9, \pi_1(1) = 0.2\}$, $\{\tau_2 = 0.7, \pi_2(1) = 0.2\}$, $\{\tau_3 = 0.5, \pi_3(1) = 0.2\}$, $\{\tau_4 = 0.3, \pi_4(1) = 0.2\}$, $\{\tau_5 = 0.1, \pi_5(1) = 0.2\}$.

Fig. 14 shows the system output y for optimal control, RLS, and BQSE, respectively. The system output for BQSE tracked the reference signal y_r and converged to the output of optimal control within about 15 iterations. Fig. 15 shows the control signal. The control signal of BQSE is closer to that of optimal control than RLS, indicating a more optimized control sequence generated from BQSE than RLS. Fig. 16 shows the convergence of Bayesian posterior probability π for BQSE. The posterior probability $\pi_5$with asymmetry parameter $\tau_5 = 0.2$ converged to 1,

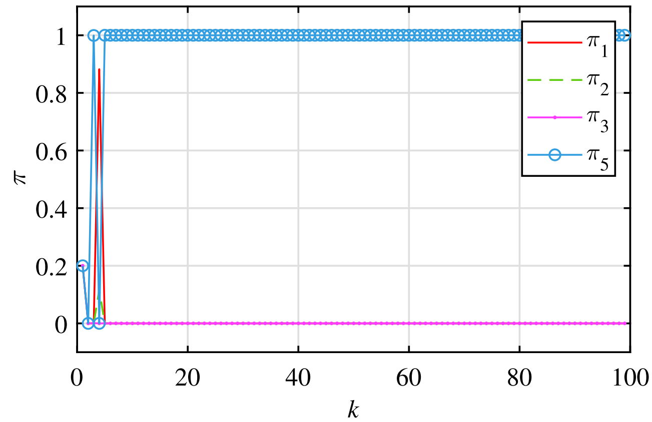

Fig. 16. The Bayesian posterior probability.

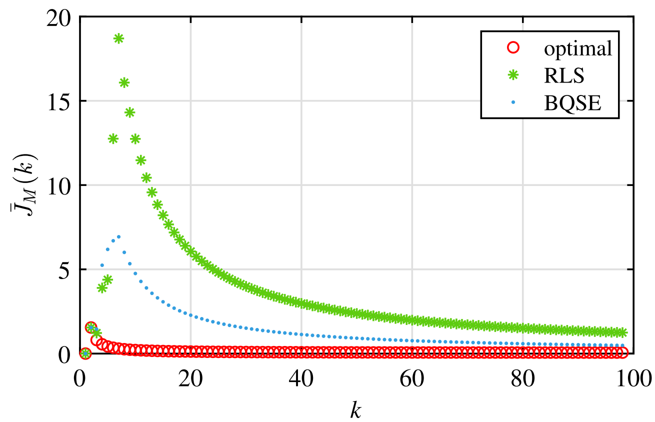

Fig. 17. The average control tracking performance index of 100 Monte Carlo simulations.

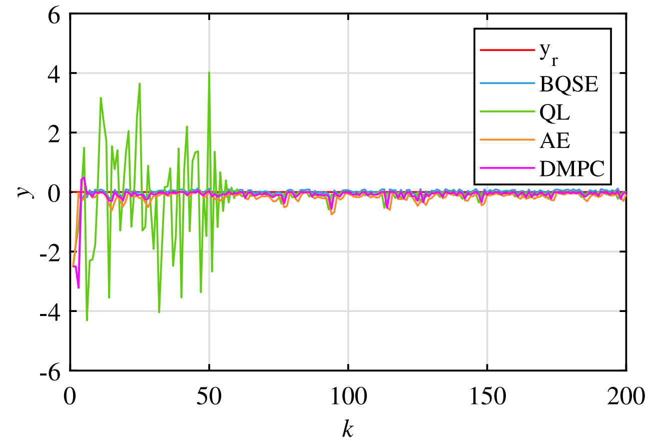

Fig. 18. The output of system with BQSE, QL, AE and DMPC.

Table 4
Comparison of three controller.

Estimation method	Average performance index
Optimal	0.0587
RLS	1.2979
BQSE	0.5032

Table 5
Comparison of four controllers.

Estimation method	Average performance index
BQSE	0.0109
QL	0.0185
AE	0.0535
DMPC	0.0174

and other posterior probabilities converged to 0 within about 15 iterations.

Fig. 17 shows the average of 100 Monte Carlo simulation results for BQSE, RLS, and optimal control in every iteration, where the evaluation criterion depicted in Eq. (40) is adopted in performance evaluation. The average tracking performance index for BQSE is closer to optimal control than RLS. Table 4 shows the average performance index for the considered control approached at the 100th iteration. The result of adaptive quantile control with BQSE is closer to the ideal strategy of optimal control than RLS, which produces a higher deviation from it.

4.4. Extensive comparison with adaptive quantile control and other approaches

In this subsection, Q-Learning based optimal tracking control (QL) [20], output error model based controller with learning adaptive estimator (AE) [23,24], and adaptive dual model predicted control (DMPC) [19] are implemented for an extensive comparison. We consider the system described in Eq. (1) with parameters the same as that in Eq. (38). Notice that Eq. (1) is converted to the state equation shown in Eq. (42) and the output error model shown in Eq. (43) to fit the calculations of the QL approach and the approach of AE, respectively.

$$\begin{aligned} \boldsymbol{x}(k+1) &= \begin{bmatrix} 0 & 1 \\ -0.7 & 2 \end{bmatrix} \boldsymbol{x}(k) + \begin{bmatrix} 1 \\ 4 \end{bmatrix} u(k) \\ y(k+1) &= [1 \quad 0]\, \boldsymbol{x}(k+1) + e(k+1) \end{aligned} \tag{42}$$

$$\begin{aligned} \begin{bmatrix} y^e(k+1) \\ y^e(k) \\ u(k) \end{bmatrix} &= \begin{bmatrix} 2 & -0.7 & 2 \\ 1 & 0 & 0 \\ 0 & 0 & 0 \end{bmatrix} \begin{bmatrix} y^e(k) \\ y^e(k-1) \\ u(k-1) \end{bmatrix} + \begin{bmatrix} 1 \\ 0 \\ 1 \end{bmatrix} u(k) \\ y(k+1) &= [1 \quad 0 \quad 0] \begin{bmatrix} y^e(k+1) \\ y^e(k) \\ u(k) \end{bmatrix} + e(k+1) \end{aligned} \tag{43}$$

The initial state is set as $y(1) = -2.5, u(1) = 0.1$ and the reference output is set as $y_r = 0$.

Fig. 18 shows the trajectories of system output y under different control methods. The QL needs long-time exploration during the start-up period. The AE needs a previous estimation for the initial parameter $H(1)$ to guarantee the convergence of the controller. Simulations in Sections 4.2 and 4.3 show that the proposed adaptive quantile control needs less adaptation period even given arbitrary initial parameters, and we set the $\theta(1)$ with offline estimation in this simulation. DMPC reduces the overshoots at the start-up period by adjusting the parameter added with dual properties. All of the control methods track the reference signal well after about 60 control iterations. To numerically analyze the experimental results, we use the performance index presented in Eq. (40) to evaluate the control performance of these controllers from 101 to 200 iterations. We conducted 100 Monte Carlo simulations and calculated the average value. The result is shown in Table 5. The BQSE obtained the lowest value, indicating that this method obtains more accurate parameter estimation and results in lower tracking error under the circumstance of ALD noise.

5. Conclusion

Our adaptive quantile control with BQSE is distinct from previous approaches, for it is the first consideration of a stochastic system with ALD noise instead of Gaussian noise as commonly considered in adaptive control. The designed BQSE provides real-time estimation of model parameters during the control process and has a more accurate estimation in the case where ALD noise is contained in system dynamics. The Bayesian posterior probability for different quantile values can converge within short execution iterations given arbitrary initial model parameters, which ultimately leads to more efficient control law derivation in adaptive control. Numerical simulations verify the parameter estimation and output tracking performances of the proposed method in stochastic system control. This control strategy can be applied in some practical cases where the system suffered from noises with peak, thick-tail, and skewed characteristics, e.g., the decision-making and macro-control for social economic systems, resource utilization and allocation of medical resources, the regulation of ecosystems.

In the future work, we plan to develop an adaptive quantile control with dual properties, where we expect to reduce the overshoots during phases of rapid adaptation, and address the challenge of measuring the parameter uncertainties for the system with ALD noises in dual control. Furthermore, the adaptive quantile control will be extended to multi-input multi-output systems for more practical cases.

Declaration of competing interest

The authors declare that they have no known competing financial interests or personal relationships that could have appeared to influence the work reported in this paper.

Acknowledgments

We acknowledge the support of National Natural Science Foundation of China grant 61773016 and 61773016.

Appendix

A.1. Cumulative distribution function for ALD

If $x < \mu$

$$\begin{aligned}\int_{-\infty}^{x} f(t)dt &= \int_{-\infty}^{x} \frac{\tau(1-\tau)}{\sigma} e^{\frac{1-\tau}{\sigma}(t-\mu)}dt \\ &= \tau e^{\frac{1-\tau}{\sigma}(t-\mu)}\Big|_{-\infty}^{x} = \tau e^{\frac{1-\tau}{\sigma}(x-\mu)}\end{aligned} \tag{44}$$

If $x \geq \mu$

$$\begin{aligned}\int_{-\infty}^{x} f(t)dt &= \int_{-\infty}^{\mu} f(t)dt + \int_{\mu}^{x} f(t)dt \\ &= \tau e^{\frac{1-\tau}{\sigma}(t-\mu)}\Big|_{-\infty}^{\mu} + \int_{\mu}^{x} \frac{\tau(1-\tau)}{\sigma} e^{\frac{-\tau}{\sigma}(t-\mu)}dt \\ &= \tau e^{\frac{1-\tau}{\sigma}(t-\mu)}\Big|_{-\infty}^{\mu} - (1-\tau)e^{\frac{-\tau}{\sigma}(t-\mu)}\Big|_{\mu}^{x} \\ &= 1-(1-\tau)e^{-\frac{\tau}{\sigma}(x-\mu)}\end{aligned} \tag{45}$$

A.2. Inverse function for ALD cumulative distribution function

If $x < \mu$, let $y = \tau e^{\frac{1-\tau}{\sigma}(x-\mu)}$, then $y \in (0, \tau)$

$$\begin{aligned}&\frac{y}{\tau} = e^{\frac{1-\tau}{\sigma}(x-\mu)} \Rightarrow \ln\frac{y}{\tau} = \frac{1-\tau}{\sigma}(x-\mu) \\ &\Rightarrow x = \mu + \frac{\sigma}{1-\tau}\ln\frac{y}{\tau}\end{aligned} \tag{46}$$

If $x \geq \mu$, let $y = 1-(1-\tau)e^{-\frac{\tau}{\sigma}(x-\mu)}$, then $y \in [\tau, 1)$

$$\begin{aligned}&\frac{1-y}{1-\tau} = e^{\frac{-\tau}{\sigma}(x-\mu)} \Rightarrow \ln\frac{1-y}{1-\tau} = \frac{-\tau}{\sigma}(x-\mu) \\ &\Rightarrow x = \mu - \frac{\sigma}{\tau}\ln\frac{1}{1-\tau}(1-y)\end{aligned} \tag{47}$$

A.3. Expectation and variance of ALD

The expectation for ALD is $E(x)$

$$\begin{aligned}E(x) &= \int_{-\infty}^{+\infty} xf(x)dx \\ &= \frac{\tau(1-\tau)}{\sigma}\left[\int_{-\infty}^{\mu} xe^{\frac{1-\tau}{\sigma}(x-\mu)}dx + \int_{\mu}^{+\infty} xe^{\frac{-\tau}{\sigma}(x-\mu)}dx\right] \\ &= \frac{\mu\tau(1-\tau)+\sigma-2\tau\sigma}{\tau(1-\tau)}\end{aligned} \tag{48}$$

when $\mu = 0$, $E(x) = \frac{\sigma(1-2\tau)}{\tau(1-\tau)}$.

The variance for ALD is $D(x)$

$$\begin{aligned}E(x^2) &= \int_{-\infty}^{+\infty} x^2 f(x)dx \\ &= \frac{\tau(1-\tau)}{\sigma}\left[\int_{-\infty}^{\mu} x^2 e^{\frac{1-\tau}{\sigma}(x-\mu)}dx + \int_{\mu}^{+\infty} x^2 e^{\frac{-\tau}{\sigma}(x-\mu)}dx\right] \\ &= \tau\mu^2 - \frac{2\sigma\tau}{1-\tau}(\mu - \frac{\sigma}{1-\tau}) + (1-\tau)\mu^2 \\ &\quad + \frac{2\sigma(1-\tau)}{\tau}(\mu + \frac{\sigma}{\tau})\end{aligned} \tag{49}$$

when $\mu = 0$, $E(x^2) = \frac{2\tau\sigma^2}{(1-\tau)^2} + \frac{2(1-\tau)\sigma^2}{\tau^2}$.

$$\begin{aligned}D(x) &= E(x^2) - E^2(x) \\ &= \frac{2\tau\sigma^2}{(1-\tau)^2} + \frac{2(1-\tau)\sigma^2}{\tau^2} - \frac{\sigma^2(1-2\tau)^2}{\tau^2(1-\tau)^2} \\ &= \frac{\sigma^2(1-2\tau+2\tau^2)}{\tau^2(1-\tau)^2}\end{aligned} \tag{50}$$

A.4. Auxiliary output

Combining system (1) and auxiliary output (6) results in

$$\begin{aligned}&z^d y_a(k) = z^d P(z^{-1})y(k) + Q(z^{-1})u(k) - z^d R(z^{-1})y_r(k) \\ &\Rightarrow z^d y_a(k) = z^d P(z^{-1})\frac{B(z^{-1})u(k-d) + C(z^{-1})e(k)}{A(z^{-1})} \\ &\qquad + Q(z^{-1})u(k) - z^d R(z^{-1})y_r(k) \\ &\Rightarrow z^d C(z^{-1})y_a(k) = \left[\frac{B(z^{-1})P(z^{-1})C(z^{-1})}{A(z^{-1})} + Q(z^{-1})C(z^{-1})\right]u(k) \\ &\qquad + z^d\frac{C(z^{-1})P(z^{-1})C(z^{-1})}{A(z^{-1})}e(k) - z^d R(z^{-1})C(z^{-1})y_r(k)\end{aligned} \tag{51}$$

Submitting $P(z^{-1})C(z^{-1}) = A(z^{-1})L(z^{-1}) + z^{-d}G(z^{-1})$ into (45)

$$\begin{aligned} z^dC(z^{-1})y_a(k) &= \left[B(z^{-1})L(z^{-1}) + Q(z^{-1})C(z^{-1})\right]u(k) + G(z^{-1})y(k) \\ &+ z^dC(z^{-1})L(z^{-1})e(k) - z^dR(z^{-1})C(z^{-1})y_r(k) \end{aligned} \tag{52}$$

The Eq. (52) can be rewritten as Eq. (7).

A.5. Recursive quantile estimation

According to Least Square, the $\hat{\boldsymbol{\theta}}$ at the kth iteration is

$$\hat{\boldsymbol{\theta}}_k = (\boldsymbol{\Phi}_k^T\boldsymbol{W}_k\boldsymbol{\Phi}_k)^{-1}\boldsymbol{\Phi}_k^T\boldsymbol{W}_k\boldsymbol{Y}_k \tag{53}$$

where

$$\boldsymbol{W}_{k-1} = \begin{bmatrix} \boldsymbol{W}_{k-1} & \cdots \\ \cdots & \tau_k \end{bmatrix} \tag{54}$$

$$\boldsymbol{\Phi}_k = \begin{bmatrix} \boldsymbol{\Phi}_{k-1} \\ \boldsymbol{\varphi}(k) \end{bmatrix} \tag{55}$$

$$\boldsymbol{Y}_k = \begin{bmatrix} \boldsymbol{Y}_{k-1} \\ y(k+1) \end{bmatrix} \tag{56}$$

Let

$$\begin{aligned} \boldsymbol{P}(k) &= [\boldsymbol{\Phi}_k^T\boldsymbol{W}_k\boldsymbol{\Phi}_k]^{-1} \\ &= [\boldsymbol{\Phi}_{k-1}^T\boldsymbol{W}_{k-1}\boldsymbol{\Phi}_{k-1} + \tau\boldsymbol{\varphi}(k)\boldsymbol{\varphi}^T(k)]^{-1} \\ &= [\boldsymbol{P}^{-1}(k-1) + \tau\boldsymbol{\varphi}(k)\boldsymbol{\varphi}^T(k)]^{-1} \end{aligned} \tag{57}$$

then Eq. (57) can be written as

$$\boldsymbol{P}^{-1}(k) = \boldsymbol{P}^{-1}(k-1) + \tau\boldsymbol{\varphi}(k)\boldsymbol{\varphi}^T(k) \tag{58}$$

According to Eqs. (53) and (57)

$$\begin{aligned} \hat{\boldsymbol{\theta}}(k-1) &= (\boldsymbol{\Phi}_{k-1}^T\boldsymbol{W}_{k-1}\boldsymbol{\Phi}_{k-1})^{-1}\boldsymbol{\Phi}_{k-1}^T\boldsymbol{W}_{k-1}\boldsymbol{Y}_{k-1} \\ &= \boldsymbol{P}(k-1)\boldsymbol{\Phi}_{k-1}^T\boldsymbol{W}_{k-1}\boldsymbol{Y}_{k-1} \end{aligned} \tag{59}$$

According to Eqs. (58) and (59)

$$\begin{aligned} \boldsymbol{\Phi}_{k-1}^T\boldsymbol{W}_{k-1}\boldsymbol{Y}_{k-1} &= \boldsymbol{P}^{-1}(k-1)\hat{\boldsymbol{\theta}}(k-1) \\ &= [\boldsymbol{P}^{-1}(k) - \tau\boldsymbol{\varphi}(k)\boldsymbol{\varphi}^T(k)]\hat{\boldsymbol{\theta}}(k-1) \end{aligned} \tag{60}$$

The estimated $\hat{\boldsymbol{\theta}}$ at the kth iteration can be written as

$$\begin{aligned} \hat{\boldsymbol{\theta}}(k) &= \boldsymbol{P}(k)\boldsymbol{\Phi}_k^T\boldsymbol{W}_k\boldsymbol{Y}_k \\ &= \boldsymbol{P}(k)[\boldsymbol{\Phi}_{k-1}^T\boldsymbol{W}_{k-1}\boldsymbol{Y}_{k-1} + \tau\boldsymbol{\varphi}(k)y(k)] \\ &= \boldsymbol{P}(k)\{[\boldsymbol{P}^{-1}(k) - \tau\boldsymbol{\varphi}(k)\boldsymbol{\varphi}^T(k)]\hat{\boldsymbol{\theta}}(k-1) + \tau\boldsymbol{\varphi}(k)y(k)\} \\ &= \hat{\boldsymbol{\theta}}(k-1) + \tau\boldsymbol{P}(k)\boldsymbol{\varphi}(k)[y(k) - \boldsymbol{\varphi}^T(k)\hat{\boldsymbol{\theta}}(k-1)] \\ &= \hat{\boldsymbol{\theta}}(k-1) + \boldsymbol{K}(k)[y(k) - \boldsymbol{\varphi}^T(k)\hat{\boldsymbol{\theta}}(k-1)] \end{aligned} \tag{61}$$

where $\boldsymbol{K}(k) = \tau\boldsymbol{P}(k)\boldsymbol{\varphi}(k)$.

Eq. (57) can be rewritten as

$$\boldsymbol{P}(k) = \boldsymbol{P}(k-1) - \frac{\tau\boldsymbol{P}(k-1)\boldsymbol{\varphi}(k)\boldsymbol{\varphi}^T(k)\boldsymbol{P}(k-1)}{\boldsymbol{I} + \tau\boldsymbol{\varphi}^T(k)\boldsymbol{P}(k-1)\boldsymbol{\varphi}(k)} \tag{62}$$

Substituting Eq. (62) into $\boldsymbol{K}(k+1)$ results in

$$\boldsymbol{K}(k) = \frac{\tau\boldsymbol{P}(k-1)\boldsymbol{\varphi}(k)}{\boldsymbol{I} + \tau\boldsymbol{\varphi}^T(k)\boldsymbol{P}(k-1)\boldsymbol{\varphi}(k)} \tag{63}$$

According to Eqs. (62) and (63), it can be obtained that

$$\boldsymbol{P}(k) = [\boldsymbol{I} - \boldsymbol{K}(k)\boldsymbol{\varphi}^T(k)]\boldsymbol{P}(k-1) \tag{64}$$

References

[1] Xiao L, Wang Z, Wu Y. Composite quantile regression estimation for left censored response longitudinal data. Acta Math Appl Sin 2018;34(4):730–41.
[2] Altunba Y, Thornton J. The impact of financial development on income inequality: A quantile regression approach. Econom Lett 2019;175:51–6.
[3] Jorion P. Value at risk : The new benchmark for managing financial risk. McGraw-Hill; 2006.
[4] DeCandia G, Hastorun D, Jampani M, Kakulapati G, Lakshman A, Pilchin A, Sivasubramanian S, Vosshall P, Vogels W. Dynamo: Amazon's highly available key-value store. SIGOPS Oper Syst Rev 2007;41(6):205–20.
[5] Benoit DF, Van den Poel D. Benefits of quantile regression for the analysis of customer lifetime value in a contractual setting: An application in financial services. Expert Syst Appl 2009;36(7):10475–84.
[6] Nguyen BT, Albrecht JW, Vroman SB, Westbrook MD. A quantile regression decomposition of urban-rural inequality in Vietnam. J Dev Econ 2007;83(2):466–90.
[7] Filatov NM, Unbehauen H. Adaptive dual control: Theory and applications. Springer Science & Business Media; 2004.
[8] Astrom KJ. Introduction to stochastic control theory. Elsevier; 1971.
[9] Maybeck PS. Stochastic models, estimation and control. Academic Press; 1979.
[10] Bertsekas DP. Dynamic programming and stochastic control. Academic Press; 1976.
[11] Clarke DW, Gawthrop PJ. Self-tuning controller. Proc Inst Electr Eng 1975;122(9):929–34.
[12] Åström KJ, Borisson U, Ljung L, Wittenmark B. Theory and applications of self-tuning regulators. Automatica 1977;13(5):457–76.
[13] Lo W, Rad A, Li C. Self-tuning control of systems with unknown time delay via extended polynomial identification. ISA Trans 2003;42(2):259–72.
[14] Orzechowski PK, Chen NY, Gibson JS, Tsao T-C. Optimal suppression of laser beam jitter by high-order RLS adaptive control. IEEE Trans Control Syst Technol 2008;16(2):255–67.
[15] Tse E, Bar-Shalom Y. Generalized certainty equivalence and dual effect in stochastic control. IEEE Trans Automat Control 1975;20(6):817–9.
[16] Zhao Y, Collins Jr EG, Cartes DA. Self-tuning adaptive control for an industrial weigh belt feeder. ISA Trans 2003;42(3):437–50.
[17] Shi J, Bo L, Yu Z. Study on self-tuning pole assignment speed control of an ultrasonic motor. ISA Trans 2011;50(4):581–7.
[18] Vasanthi D, Pranavamoorthy B, Pappa N. Design of a self-tuning regulator for temperature control of a polymerization reactor. ISA Trans 2012;51(1):22–9.
[19] Cao W, Li S. Enhanced parameterizable uncertainty to dual adaptive model predictive control. Control Theory Appilcation 2019;36(8):1197–206.
[20] Kiumarsi B, Lewis FL, Modares H, Karimpour A, Naghibi-Sistani M-B. Reinforcement Q-learning for optimal tracking control of linear discrete-time systems with unknown dynamics. Automatica 2014;50(4):1167–75.
[21] Kiumarsi B, Lewis FL, Naghibi-Sistani M-B, Karimpour A. Optimal tracking control of unknown discrete-time linear systems using input-output measured data. IEEE Trans Cybern 2015;45(12):2770–9.
[22] Kiumarsi B, Lewis FL. Actor-critic-based optimal tracking for partially unknown nonlinear discrete-time systems. IEEE Trans Neural Netw Learn Syst 2014;26(1):140–51.
[23] Tutsoy O, Colak S. Adaptive estimator design for unstable output error systems: A test problem and traditional system identification based analysis. Proc Inst Mech Eng I J Syst Control Eng 2015;229(10):902–16.
[24] Tutsoy O. Design and comparison base analysis of adaptive estimator for completely unknown linear systems in the presence of OE noise and constant input time delay. Asian J Control 2016;18(3):1020–9.
[25] Zames G. Feedback and optimal sensitivity: Model reference transformations, multiplicative seminorms, and approximate inverses. IEEE Trans Automat Control 1981;26(2):301–20.
[26] Van Der Schaft AJ. L_2-Gain analysis of nonlinear systems and nonlinear state feedback H_∞ control. IEEE Trans Autom Control 1992;37(6):770–84.
[27] Başar T, Bernhard P. H-infinity optimal control and related minimax design problems: A dynamic game approach. Springer Science & Business Media; 2008.
[28] Al-Tamimi A, Lewis FL, Abu-Khalaf M. Model-free Q-learning designs for linear discrete-time zero-sum games with application to H-infinity control. Automatica 2007;43(3):473–81.
[29] Al-Tamimi A, Abu-Khalaf M, Lewis FL. Adaptive critic designs for discrete-time zero-sum games with application to H_∞ control. IEEE Trans Syst Man Cybern B 2007;37(1):240–7.
[30] Kiumarsi B, Lewis FL, Jiang Z. H_∞ Control of linear discrete-time systems: Off-policy reinforcement learning. Automatica 2017;78:144–52.
[31] Valadbeigi AP, Sedigh AK, Lewis FL. H_∞ Static output-feedback control design for discrete-time systems using reinforcement learning. IEEE Trans Neural Netw Learn Syst 2020;31(2):396–406.

[32] Jiang Y, Kiumarsi B, Fan J, Chai T, Li J, Lewis FL. Optimal output regulation of linear discrete-time systems with unknown dynamics using reinforcement learning. IEEE Trans Cybern 2020;50(7):3147–56.
[33] Zhao K, Lian H. The expectation–maximization approach for Bayesian quantile regression. Comput Statist Data Anal 2016;96(1):1–11.
[34] Yu K, Moyeed RA. Bayesian Quantile regression. Statist Probab Lett 2001;54(4):437–47.
[35] Lancaster T, Jun SJ. Bayesian Quantile regression methods. J Appl Econometrics 2010;25(2):287–307.
[36] Ordiano JÁG, Gröll L, Mikut R, Hagenmeyer V. Probabilistic energy forecasting using the nearest neighbors quantile filter and quantile regression. Int J Forecast 2020;36(1):310–23.
[37] Fan Y, Liu R. Partial identification and inference in censored quantile regression. J Econometrics 2018;206:1–55.
[38] Hallock KF, Koenker RW. Quantile regression. J Econ Perspect 2001;15(4):143–56.
[39] Koenker R. Quantile regression for longitudinal data. J Multivariate Anal 2004;91(1):74–89.
[40] Wang H, Li C. Distributed quantile regression over sensor networks. IEEE Trans Signal Inf Process Netw 2018;4(2):338–48.
[41] Zou H, Yuan M, et al. Composite quantile regression and the oracle model selection theory. Ann Statist 2008;36(3):1108–26.
[42] Zhao Z, Xiao Z. Efficient regressions via optimally combining quantile information. Econometric Theory 2014;30(6):1272.
[43] Huang H, Chen Z. Bayesian composite quantile regression. J Stat Comput Simul 2015;1(1):1–14.
[44] Kozubowski TJ, Podgorski K. Asymmetric Laplace distributions. Math Sci 2000;25(1):37–46.
[45] Roger K. Quantile regression. Cambridge University Press; 2005.
[46] Van de Water H, Willems J. The certainty equivalence property in stochastic control theory. IEEE Trans Automat Control 1981;26(5):1080–7.
[47] Karafyllis I, Krstic M. Adaptive certainty-equivalence control with regulation-triggered finite-time least-squares identification. IEEE Trans Automat Control 2018;63(10):3261–75.
[48] Boskovic JD, Han Z. Certainty equivalence adaptive control of plants with unmatched uncertainty using state feedback. IEEE Trans Automat Control 2009;54(8):1918–24.